

Quantum evaporation from superfluid helium at normal incidence

This article has been downloaded from IOPscience. Please scroll down to see the full text article.

1997 J. Phys.: Condens. Matter 9 L369

(<http://iopscience.iop.org/0953-8984/9/24/004>)

View [the table of contents for this issue](#), or go to the [journal homepage](#) for more

Download details:

IP Address: 171.66.16.207

The article was downloaded on 14/05/2010 at 08:56

Please note that [terms and conditions apply](#).

LETTER TO THE EDITOR

Quantum evaporation from superfluid helium at normal incidenceF Dalfovo[†], M Guilleumas[†], A Lastri[†], L Pitaevskii[‡] and S Stringari[†][†] Dipartimento di Fisica, Università di Trento, I-38050 Povo, Italy[‡] Department of Physics, Technion, Haifa 32000, Israel, and Kapitza Institute for Physical Problems, ul. Kosygina 2, 117334 Moscow, Russia

Received 6 December 1996

Abstract. We study the scattering of atoms, rotons and phonons at the free surface of ⁴He at normal incidence and calculate the evaporation, condensation and reflection probabilities. Assuming elastic one-to-one processes and using general properties of the scattering matrix, such as unitarity and time reversal, we argue that all nonzero probabilities can be written in terms of a single energy-dependent parameter. Quantitative predictions are obtained using linearized time-dependent density functional theory.

Superfluid helium at low temperature exhibits the peculiar phenomenon of quantum evaporation. Elementary excitations, such as rotons and high-energy phonons, propagate in the liquid with long mean free path and with an energy which can exceed the binding energy of atoms in the liquid. Thus, when an elementary excitation impinges upon the free surface it may eject an atom from the liquid through a quantum process. The scattering of excitations and atoms at the free surface of the superfluid have been extensively studied in recent years (see for instance [1]–[3] and references therein), but the comparison between theory and experiments is still unsatisfactory. Previous theoretical approaches to the problem of quantum evaporation made use of semiclassical approximations [4, 5]. Recently [6, 7] we have calculated the probability of evaporation, condensation and reflection of rotons and atoms using a time-dependent density functional (TDDF) theory. The density functional has proven to be a powerful method to investigate various structural features of inhomogeneous superfluid helium [8] including static and dynamic properties of the free surface, droplets and films. When applied to quantum evaporation, the linearized TDDF theory accounts only for one-to-one processes, but includes quantum effects beyond the semiclassical approximation. So far we have restricted the analysis to the phonon forbidden region [6, 7], corresponding to incidence angles such that phonons are excluded by energy and momentum conservation. In the present work we apply the same theory to the case of scattering at normal incidence, where atoms and rotons as well as phonons take part in the scattering processes. We show that the complexity of the scattering processes is dramatically reduced on the basis of simple arguments based on symmetry properties of the scattering matrix and threshold effects. The final result is that all nonzero probabilities can be expressed in terms of a single energy-dependent parameter. The numerical solution of the TDDF equations confirms this picture and provides quantitative predictions for the probabilities as a function of energy.

In figure 1 we show the phonon–roton dispersion curve in bulk liquid. The phonon branch goes from $q = 0$ up to the maxon (Δ^*). On the right of the maxon the slope is negative and corresponds to the dispersion of R^- rotons, that is, rotons with negative group

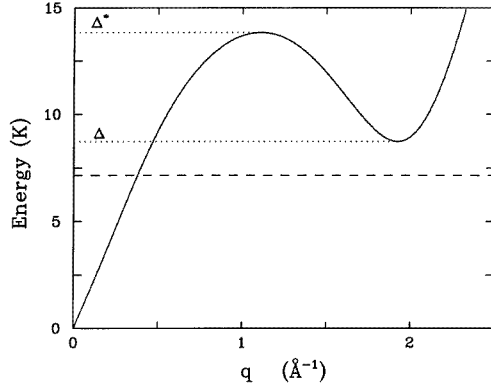


Figure 1. Phonon-roton dispersion in liquid ^4He . The dashed line is the threshold $|\mu| = 7.15$ K for atom evaporation.

velocity. Then the slope becomes positive again for R^+ rotons on the right of the roton minimum (Δ). The threshold for atom evaporation at normal incidence coincides with the chemical potential, $|\mu| = 7.15$ K (dashed line): only excitations with energy higher than $|\mu|$ can produce quantum evaporation. The energy of an evaporated atom is simply $|\mu| + \hbar^2 q^2 / 2m$. For scattering at normal incidence, the problem is unidimensional; the wave vector \mathbf{q} is orthogonal to the free surface and is not a conserved quantity, since the surface breaks translational invariance. As already said, we consider elastic processes in which the energy $\hbar\omega$ is conserved.

Four types of excitation interact at the free surface of the superfluid: atoms (a), phonons (p) and rotons with positive (+) and negative (-) group velocity. One can define the scattering matrix by means of $\Psi_{out} = S\Psi_{in}$, where Ψ_{in} and Ψ_{out} are the incoming and outgoing asymptotic solutions, respectively. The matrix element S_{ij} connects a particular input (i) and output (j) channel, with $i, j = a, p, +, -$, and depends on energy and incident angle. It determines the probability associated with each scattering process by $P_{ij} = |S_{ij}|^2$. These channels correspond to atom, phonon and roton excitation states. Thus, there are 16 complex scattering matrix elements S_{ij} , and hence 16 probabilities P_{ij} , to be determined. The unitarity and the time reversal symmetry ($t \rightarrow -t$) of S imply $S^\dagger = S^{-1}$ and $S^* = S^{-1}$, respectively. Combining these two conditions one finds that the scattering matrix elements must satisfy the general property $S_{ij} = S_{ji}$, reducing the number of independent matrix elements to ten. Furthermore, the unitarity condition $S^*S = 1$ gives ten additional constraints. For instance, if the incident excitation is of type i , then one has the unitarity conditions

$$\sum_j |S_{ij}|^2 = 1 \quad (1)$$

where $i, j = a, p, +, -$, yielding four linear combinations of matrix elements. The other six conditions are

$$S_{aa}^* S_{ap} + S_{ap}^* S_{pp} + S_{a-}^* S_{-p} + S_{a+}^* S_{+p} = 0 \quad (2)$$

$$S_{aa}^* S_{a-} + S_{ap}^* S_{p-} + S_{a-}^* S_{--} + S_{a+}^* S_{+-} = 0 \quad (3)$$

$$S_{aa}^* S_{a+} + S_{ap}^* S_{p+} + S_{a-}^* S_{-+} + S_{a+}^* S_{++} = 0 \quad (4)$$

$$S_{pa}^* S_{a-} + S_{pp}^* S_{p-} + S_{p-}^* S_{--} + S_{p+}^* S_{+-} = 0 \quad (5)$$

$$S_{pa}^* S_{a+} + S_{pp}^* S_{p+} + S_{p-}^* S_{-+} + S_{p+}^* S_{++} = 0 \quad (6)$$

$$S_{-a}^* S_{a+} + S_{-p}^* S_{p+} + S_{--}^* S_{-+} + S_{-+}^* S_{++} = 0. \quad (7)$$

We will now combine these rigorous relations with further arguments about threshold effects and momentum exchange at the surface in order to reduce the number of relevant unknowns.

The roton minimum represents the threshold energy to excite R^- and R^+ rotons in the liquid. These excitations coincide at Δ and, on the basis of symmetry arguments, one can prove [9] that the mode-change reflection between R^- and R^+ is the dominant one just above Δ ($P_{+-} \simeq 1$) and that the other probabilities involving R^- and R^+ are small. Conversely, below it only phonons and atoms are present. Among the different processes the phonon \leftrightarrow atom scattering is expected to be favoured ($P_{pa} \simeq 1$), since it implies the smallest change of momentum. In fact, the normal reflection of a phonon or an atom would imply a much larger momentum transferred to the surface and this seems unlikely for a smooth surface such as that of helium, except near the threshold $\hbar\omega \simeq |\mu|$ where the atom momentum goes to zero and full reflection takes place. Now, assuming $P_{+-} \simeq 1$ and $P_{pa} \simeq 1$ in the unitarity conditions (1), one finds that all the remaining probabilities should vanish close to Δ .

Similarly, the maxon is a threshold for phonons and R^- rotons and one expects the mode-change reflection between R^- and phonons to dominate just below Δ^* ($P_{p-} \simeq 1$). Just above it, one has only R^+ and atoms. For the same argument of smallest momentum transferred to the surface, the $R^+ \leftrightarrow$ atom scattering should be greatly favoured ($P_{+a} \simeq 1$) with respect to the normal reflection of rotons and atoms. Putting $P_{p-} \simeq 1$ and $P_{+a} \simeq 1$ in the unitarity conditions one finds again that the other probabilities have to vanish near Δ^* .

The above arguments suggest that P_{pa} and P_{+-} decrease from unity to zero on increasing the energy from Δ to Δ^* , while P_{p-} and P_{+a} increase from zero to unity in the same range. All probabilities should be smooth functions of the energy. Those that are zero at both Δ and Δ^* are expected to be small everywhere in between. If we make the assumption that they vanish for any value of energy ($\Delta \leq \hbar\omega \leq \Delta^*$)

$$P_{aa} = P_{pp} = P_{--} = P_{++} = P_{-a} = P_{+p} = 0 \quad (8)$$

we find simple and useful relations among the remaining nonzero probabilities. In fact, by inserting assumption (8) into the unitarity conditions (1)–(7), after some simple algebra one obtains [10]

$$P_{pa} = P_{+-} = 1 - P_{p-} = 1 - P_{+a}. \quad (9)$$

This means that all nonzero probabilities at normal incidence can be written in terms of a single parameter. This result is expected to hold for any theory accounting only for one-to-one elastic processes.

In the remaining part of the paper we show that the numerical calculation of P_{ij} , within TDDF theory, is consistent with the general properties of the scattering matrix and with the threshold effect near Δ and Δ^* . Furthermore, it confirms the validity of assumption (8).

In order to calculate explicitly the probabilities P_{ij} one needs a theory for the elementary excitations of the nonuniform liquid. The theory must provide a spectrum of elementary excitations close to the experimental one, since the proper energy balance between the excitations is crucial; moreover, it must allow one to calculate the asymptotic flux of elementary excitations in a given process, in order to extract the corresponding matrix elements.

In a density functional approach [6, 7] one assumes the energy of the system to be in the form $E = \int dr \mathcal{H}[\Psi, \Psi^*]$, where the complex function $\Psi = \Phi \exp(iS/\hbar)$ is related to the density and velocity of the superfluid by means of $\rho = \Phi^2$ and $v = (1/m) \nabla S$. We use a phenomenological energy density \mathcal{H} [8] which has been adjusted to provide an

accurate description of the equation of state, the static response function and the phonon–roton dispersion law of the bulk liquid. The description of the functional can be found in our previous papers [7, 8].

The eigenenergies and eigenfunctions of the system are calculated within a TDDF approach. The propagation of the elementary excitations is described by linearizing the wave function around the ground state $\Psi_0(\mathbf{r})$:

$$\Psi(\mathbf{r}, t) = \Psi_0(\mathbf{r}) + \delta\Psi(\mathbf{r}, t). \quad (10)$$

Far away from the surface $\delta\Psi(\mathbf{r}, t)$ corresponds to the propagation of phonons and rotons in the liquid and free atoms in the vacuum. Due to linearization, only one-to-one processes are taken into account. Thus the theory cannot describe inelastic processes, such as decay into multi-ripples or multi-phonons.

For practical reasons we work in a slab geometry. The semi-infinite system is simulated by slabs of liquid with thickness ranging from 50 to 100 Å, and centred in a finite box whose size is of the order of 100–150 Å. The density functional provides also the ground state density profile of the liquid as the stationary solution of lowest energy. The profile of the liquid–vacuum interface has a thickness of about 6 Å and a shape close to that obtained with *ab initio* Monte Carlo calculations (see [8] for details). Choosing z along the normal to the surface, one can write the wave function $\delta\Psi$ in the form

$$\delta\Psi(z, t) = f(z) e^{-i\omega t} + g(z) e^{i\omega t}. \quad (11)$$

The quantities $f(z)$ and $g(z)$ are real functions, which have to be determined, together with ω , by solving self-consistently the equations of motion

$$\delta \int dt \int d\mathbf{r} \left\{ \mathcal{H}[\Psi, \Psi^*] - \mu \Psi \Psi^* - \Psi^* i\hbar \frac{\partial \Psi}{\partial t} \right\} = 0 \quad (12)$$

linearized with respect to f and g . Equations (11) and (12) assume the typical form of the random phase approximation (RPA) for bosons. In the formalism of the RPA, $f(z)$ and $g(z)$ take into account the particle–hole and hole–particle transitions, respectively. The two components f and g of the excited states are coupled by the equations of motion (12).

We have solved numerically the linearized TDDF equations in the finite box, obtaining a set of discrete eigenenergies ω and the corresponding eigenfunctions $f(z)$ and $g(z)$. For a given ω , the solution is a stationary state. Inside the slab, $f(z)$ and $g(z)$ are oscillating functions associated with the propagation of phonons and rotons, whose dispersion law is shown in figure 1. Outside the slab, where particles are uncorrelated, the function $g(z)$ vanishes while the equation for $f(z)$ coincides with the Schrödinger equation for free atoms. By looking at the Fourier transforms of the signal far away from the surface, both inside and outside the slab, one can evaluate the asymptotic amplitudes (f_i and g_i) and the momentum q_i of each type of excitation which contributes to $\delta\Psi$. A fitting procedure has been used in order to extract the numerical values of f_i and g_i needed for the analysis of the evaporation rates.

A given scattering process at a certain energy can be obtained as a linear combination of different stationary solutions at that energy. The latter can be found by slightly varying the slab thickness (L_{slab}) and the box size (L_{box}). Then, one can evaluate the flux of incoming and outgoing excitations. In the present linearized TDDF theory, the current associated with a given elementary excitation is

$$\mathbf{j}_i = \mathbf{v}_i (|f_i|^2 - |g_i|^2) \quad (13)$$

where \mathbf{v} is its group velocity. From the asymptotic fluxes one can easily evaluate the evaporation, condensation and reflection probabilities [7].

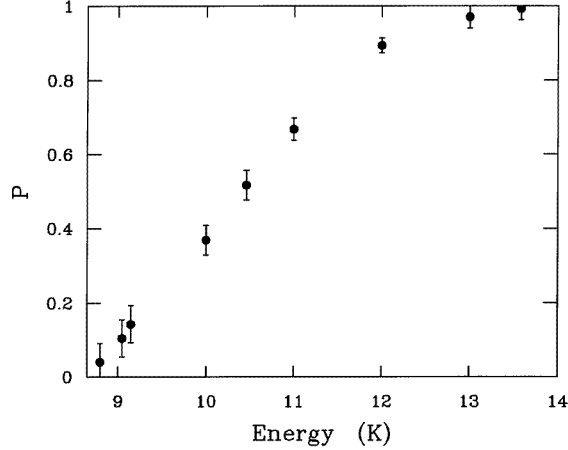


Figure 2. Probability $P \equiv P_{+a}$ as a function of energy. The other nonzero probabilities can be extracted using (9). The energy scale starts from Δ .

We have first verified that the resulting probabilities P_{ij} satisfy, within the accuracy of the calculation, the symmetry property $P_{ij} = P_{ji}$ and the unitarity conditions (1) in the whole range of energy $\hbar\omega > |\mu|$. Explicit results are shown in table 1 for an intermediate value of energy ($\hbar\omega = 11$ K). Four states at the same energy are combined to describe the scattering processes (atom \rightarrow atom, phonon, R^- , R^+), (phonon \rightarrow atom, phonon, R^- , R^+), ($R^+ \rightarrow$ atom, phonon, R^- , R^+) and ($R^- \rightarrow$ atom, phonon, R^- , R^+). The numerical uncertainty, which is less than ± 0.05 for all probabilities, originates mainly from the fact that the states in the linear combinations may be not sufficiently linearly independent [7].

Table 1. Probabilities P_{ij} for four different scattering processes (incident atom, phonon, R^- and R^+ , respectively) described by linear combinations of four states at the same energy (11 K) and for different values of (L_{slab}, L_{box}) . The unitarity condition, (1), is labelled by Σ .

Incident exc.	P_{ij}				Σ
Atom	$P_{aa} = 0.0002$	$P_{ap} = 0.3384$	$P_{a-} = 0.0003$	$P_{a+} = 0.6837$	1.0226
Phonon	$P_{pa} = 0.3236$	$P_{pp} = 0.0020$	$P_{p-} = 0.6487$	$P_{p+} = 0.00002$	0.9743
R^-	$P_{-a} = 0.0004$	$P_{-p} = 0.6859$	$P_{--} = 0.0013$	$P_{-+} = 0.3408$	1.0284
R^+	$P_{+a} = 0.6537$	$P_{+p} = 0.0001$	$P_{+-} = 0.3222$	$P_{++} = 0.00002$	0.9760

We find also that the probabilities P_{aa} , P_{pp} , P_{--} , P_{++} , P_{-a} , and P_{p+} are extremely small at all energies; they turn out to be zero within the present accuracy, confirming the hypothesis (8) made before. Furthermore, the nonzero probabilities turn out to verify relations (9). It is therefore possible to resume all the information about the nonzero probabilities in a single function of energy, $P(\omega)$. Let us call $P(\omega) \equiv P_{+a}$. This quantity is plotted in figure 2, in the energy range $\Delta \leq \hbar\omega \leq \Delta^*$. The probability of mode-change scattering between R^- and phonons (P_{p-}) is equal to the evaporation probability for R^+ rotons (P_{+a}); both probabilities start from zero at the roton minimum and increase to unity at the maxon energy. The evaporation probability for R^+ rotons is equal to unity even above the maxon energy. The evaporation probability for phonons (P_{pa}) is equal to that for the mode-change process between rotons (P_{+-}). They are equal to $(1 - P_{+a})$, so they decrease from unity to zero

between Δ and Δ^* . It is worth noting that the present results for the evaporation probability P_{+a} at normal incidence coincide, within the error bar, with those obtained previously in the phonon forbidden region [7], that is, for R^+ rotons impinging at about $15\text{--}20^\circ$. The same is true for the mode-change probability P_{+-} [11].

Only a few experimental estimates are available for the probabilities P_{ij} . Indeed, by measuring time-of-flight and angular distributions of evaporated atoms, one-to-one evaporation processes have been clearly seen [1], but a quantitative determination of the ratio between incoming and outgoing fluxes, and hence P_{ij} , is difficult. There are evidences for a sizable probability P_{+a} , which should increase with a trend similar to that in figure 1 [12]. A recent estimate [13] of the phonon \rightarrow atom probability, for high-energy phonons ($\hbar\omega > 10$ K), is $P_{pa} \simeq 0.1$. Our theory, in the same range of energy, gives a value which decreases rapidly from 0.5 to 0. We also find that an incident atom condenses with probability $P_{ap} + P_{a+} \simeq 1$ and hence the reflection probability P_{aa} is almost zero. This is in agreement with the observed small reflectivity [2, 3]; but the experiments also support the idea that the atom condensation might occur through processes such as two-phonon or multi-rippylon production. The extension of the present formalism to include such mechanisms, beyond the one-to-one hypothesis, remains an important task, for a more systematic comparison between theory and experiments.

MG thanks the Generalitat de Catalunya for financial support.

References

- [1] Brown M and Wyatt A F G 1990 *J. Phys.: Condens. Matter* **2** 5025
- [2] Wyatt A F G, Tucker M A H and Cregan R F 1995 *Phys. Rev. Lett.* **74** 5236
- [3] Edwards D O 1982 *Physica B* **109/110** 1531, and references therein
Nayak V V, Edwards D O and Masuhara N 1983 *Phys. Rev. Lett.* **50** 990
Mukherjee S, Candela D, Edwards D O and Kumar S 1987 *Japan. J. Appl. Phys.* **26** 257
- [4] Maris H J 1992 *J. Low Temp. Phys.* **87** 773
- [5] Mulheran P A and Inkson J C 1992 *Phys. Rev. B* **46** 5454
- [6] Dalfovo F, Fracchetti A, Lastri A, Pitaevskii L and Stringari S 1995 *Phys. Rev. Lett.* **75** 2510
- [7] Dalfovo F, Fracchetti A, Lastri A, Pitaevskii L and Stringari S 1996 *J. Low Temp. Phys.* **104** 367
- [8] Dalfovo F, Lastri A, Pricapenko L, Stringari S and Treiner J 1995 *Phys. Rev. B* **52** 1193
- [9] Lastri A, Dalfovo F, Pitaevskii L and Stringari S 1995 *J. Low Temp. Phys.* **98** 227
- [10] For a similar procedure applied in the phonon forbidden region see [7] or Dalfovo F, Pitaevskii L and Stringari S 1996 *Proc. LT21 Conf.; Czech. J. Phys.* **46-S1** 391
- [11] Stringari S, Dalfovo F, Guilleumas M, Lastri A and Pitaevskii L 1996 *Proc. LT21 Conference; Czech. J. Phys.* **46-S6** 2973
- [12] Forbes A C and Wyatt A F G 1995 *J. Low Temp. Phys.* **101** 537 Forbes A C and Wyatt A F G private communication
- [13] Tucker M A H and Wyatt A F G 1996 *Czech. J. Phys.* **46** 263